Understanding key limiting factors for the development of all-solid-state-batteries

Yim, Chae-Ho; Houache, Mohamed S.E.; Baranova, Elena A.; Abu-Lebdeh, Yaser

Publisher's version / Version de l'éditeur:
https://doi.org/10.1016/j.ceja.2022.100436
Chemical Engineering Journal Advances, 13, pp. 1-7, 2022-12-15

Chemical Engineering Journal Advances 13 (2023) 100436

Contents lists available at ScienceDirect

Chemical Engineering Journal Advances

journal homepage: www.sciencedirect.com/journal/chemical-engineering-journal-advances

Understanding key limiting factors for the development of all-solid-state-batteries

Chae-Ho Yim [a,b], Mohamed S.E. Houache [a], Elena A. Baranova [b], Yaser Abu-Lebdeh [a,*]

[a] Energy, Mining, and Environment Research Centre, National Research Council of Canada, 1200 Montreal Road, Ottawa, Ontario. K1A0R6, Canada

[b] Department of Chemical and Biological Engineering, Centre for Catalysis Research and Innovation (CCRI), University of Ottawa, 161 Louis-Pasteur, Ottawa, ON, K1N6N5, Canada

ARTICLE INFO

Keywords:
All-solid-state-battery
Li-ion
Li metal
Ultrathin lithium
Anode-free
Solid electrolyte

ABSTRACT

The All-Solid-State-Battery (ASSB) is projected to offer higher energy density and enhanced safety compared to the current commercial Li-ion battery. In this study, we have used a simple model to evaluate the effect of different cell components on the battery's overall performance. We critically examine the promised 100% increase (vs. a standard Li-ion battery) in the overall energy density of an ASSB— a claim often made in both the literature and industry. Through a survey of cell parameters possible with current technology, we were able to evaluate optimum parameters that can be expected in future ASSBs. Herein, we identify three critical parameters required to reach the promised energy density: (1) minimize the thickness of the solid electrolyte to less than 20 μm; (2) modify the cathode formulation to minimize the amount of catholyte and optimize the electrode thickness; and (3) minimize the N/P ratio by developing cells that are anode-free or utilize ultrathin lithium anodes. In conclusion, we believe that the often-cited 100% improvement in energy density for ASSBs is overly optimistic. Instead, a 30% improvement is a more reasonable target for the near future.

1. Introduction

All-solid-state batteries (ASSBs) use solid electrolytes (SEs) to replace flammable liquid electrolytes (LE) resulting in safer batteries with increased energy density enabled by the lithium metal anode. Despite the breakthroughs at the material and cell level, there are still various challenges to overcome besides the grand challenge of manufacturing these types of batteries without altering current manufacturing processes at lower costs (< 100$/KWh). The electric vehicle market continues to drive the research on ASSBs and there has been a major push to introduce the technology into the market through partnerships between ASSB developers and major original equipment manufacturers (OEM) with ambitious Start of Production (SOP) goals before 2025.

The promised increase in energy density of ASSBs is often quoted at 100% in volumetric and gravimetric values compared to Li-ion batteries (200 Wh/Kg or 400 Wh/l) when ultra-thin lithium is used. [1] For this to happen it is important to investigate all the changes that need to be made at the material and cell level compared to what is used in Li-ion cells (used herein as a baseline). This work focuses on the following limiting parameters: the thickness of the SE, anode and cathode materials; N/P ratio; and amount of cathode active materials. In general, a SE has 10 to 100 times lower ionic conductivity (10^{-4} to 10^{-3} S/cm) compared to a LE (10^{-2} S/cm). The commercial battery uses a 20 μm separator with a LE, and to perform the same for ASSBs the thickness of the SE needs to be less than 20 μm if the remaining components in the battery stay the same (which is also a major challenge depending on the class of the SE). There are three classes of SEs: inorganic, polymer, and composite (hybrid) solid electrolytes. [2–5] Inorganic solid electrolytes (ISEs) generally have a lower ionic conductivity than LEs and researchers have explored ISEs comparable to or higher than LEs. [6–10] ISEs have excellent mechanical properties and can be made thinner than 20 μm. However, their brittleness, interface resistance, and chemical instability in air, moisture, and lithium have hindered their application in ASSBs. [11–18] Solid polymer electrolytes (SPEs) are another type that use a high molecular weight polymer that can solvate a lithium salt. [2, 5, 19] The electrolyte Poly-ethylene-oxide (PEO) was first introduced by Michel Armand as a suitable electrolyte for the early generation of Li-ion batteries. [20–22] PEO electrolyte is easy to mass produce as a film and easy to utilize in roll-to-roll processes. In addition, it has better electrode/electrolyte interfacial resistance compared to the ISE. [23] Nevertheless, even though it is currently used in commercial batteries produced by Blue solutions in Canada and France for niche applications,

* Corresponding author.
E-mail address: Yaser.Abu-Lebdeh@cnrc-nrc.gc.ca (Y. Abu-Lebdeh).

https://doi.org/10.1016/j.ceja.2022.100436
Received 8 November 2022; Received in revised form 2 December 2022; Accepted 13 December 2022
Available online 15 December 2022

its mass-market penetration is heavily hindered by the low conductivity (10^{-6} – 10^{-8} S cm^{-1}) at room temperature. [24, 25] To improve the conductivity at room temperature, additives such as succinonitriles have been studied. However, the increase in conductivity with the additives gives rise to poor mechanical and thermal properties. [19] As a result, composite (or hybrid) solid electrolytes (CPEs) are suggested to maximize the advantages and minimize the disadvantages of ISEs and SPEs [2, 5, 16, 26-28]. Nevertheless, the fabrication of thin SEs is difficult. [29] Moreover, the reactivity of lithium towards ISEs and SPEs is another challenge that needs to be overcome. [26]

The projected 100% increase in energy density of ASSBs depends on the use of a lithium metal anode. However, the traditional assumption that dendrites will have more difficulty penetrating through the SE upon cycling is not entirely correct. [1, 30, 31] Nevertheless, lithium is a light metal with a high specific capacity (3.8 Ah/g) that is 10 times higher than that of the commercial graphite anode. Park et al. claim that using 190% excess Li metal as an anode decreases the volumetric energy density below that of a graphite anode. Therefore the benefits of high energy density are offset when using excess Li metal. [32] In principle, the lithium that shuttles between cathode and anode originates from the cathode, which suggests that any amount of lithium in the lithium metal anode will always be in excess. One approach to reduce the dead-weight associated with excess lithium is the use of an ultra-thin lithium anode with a thickness of less than 50 µm. [33] Moreover, the N/P ratio (capacity ratio of negative to positive) needs to be optimized for the lithium metal anode with the consideration of Coulombic efficiency, 99% [34], to maximize the energy density and durability. Another approach is an anode-free, “anode-less”, Li-ion battery [32, 35-37] that uses no or very thin layer of anode materials where N/P is close to 0, which can maximize the energy density. Lee et al. [37]. succeeded to use a Ag-C layer to control the lithium plating and stripping for 1000 cycles. The thickness of the Ag-C layer was 10 µm which is smaller than the cathode capacity used in the studies that result in lithium plating and stripping during cycling. Yan et al. have also shown an anode-free concept by coating the copper electrode with a 2D boron nitride layer that results in lithium dendrites-free cycling. [38]

The ASSB cathode has only 60 to 85 wt% of cathode active material (CAM) due to the addition of SE to aid ionic conductivity. [2, 5, 37, 39, 40] The addition of SE in the cathode electrode increases the inactive material volume and mass, which lowers the energy density and is one of the limiting factors to improving the energy density. [41] The amount of CAM in a commercial battery range from 95 to 98% to maximize the energy density of the cell. The only way to compensate for the lower CAM in ASSBs is thicker electrodes, however, the study by Du et al. [42]. has shown that thick electrodes show lower power densities due to the limitation of the lithium diffusion in LEs. However, considering the lower ionic conductivity of most SEs, the cathode thickness would have a more severe effect on the power density.

The limiting factors studied in this work are (1) SE thickness, (2) N/P ratio that also corresponds to (2a) lithium metal thickness, (2b) cathode thickness, and (2c) cathode active material volume. Fig. 1 shows the schematic of the battery and is used as the basis for evaluating the stack energy density using Eq. (1) from our previous work. [43] The energy of an active material is evaluated by multiplying the capacity by the voltage. However, the battery also contains inactive materials such as the casing, electrodes and separator. To find the influence of the inactive materials on the overall density of the battery, Obrovac et al. [44]. derived an equation for the stack energy density using the thickness of the cathode, anode, separator and current collector. The equation summarizes the dilution of the energy density due to the inactive materials. Their study concentrated on the effect of the average voltage and the capacity of the anode, while the rest of the parameters were held constant (such as the cathode thickness and the type of materials). In our previous work, we have applied the equation to study the effect of the changes in the silicon composite with changing the materials of the cathode to optimize the overall stack energy density. [43] The parameters optimized in our previous study were irreversible capacity, the energy density of the cathode, and the composition of the anode. In this study, we used the equation to study the change of all parameters except the thickness of the current collector to identify the limiting factors that influence the solid-state battery performance. The parameters are as described below and Table 1 shows the parameters used for the studies unless it is the factors of interest. The percent improvements are compared to the stack energy density when NMC and graphite are used and parameters are also shown in Table 1. Eq. (1) does not include the thickness of the anode since it depends on the N/P ratio and the thickness of the cathode. *Eq. (2)* shows the volumetric reversible capacity of the electrode that depends on the percentage of the active material volume in the electrodes. Due to the limitation of the equation, the type of the solid electrolyte is not discussed in this work. Only the thickness dependency of the solid electrolyte is discussed. Furthermore, due to the focus of this theoretical work on the energy density, the cycle

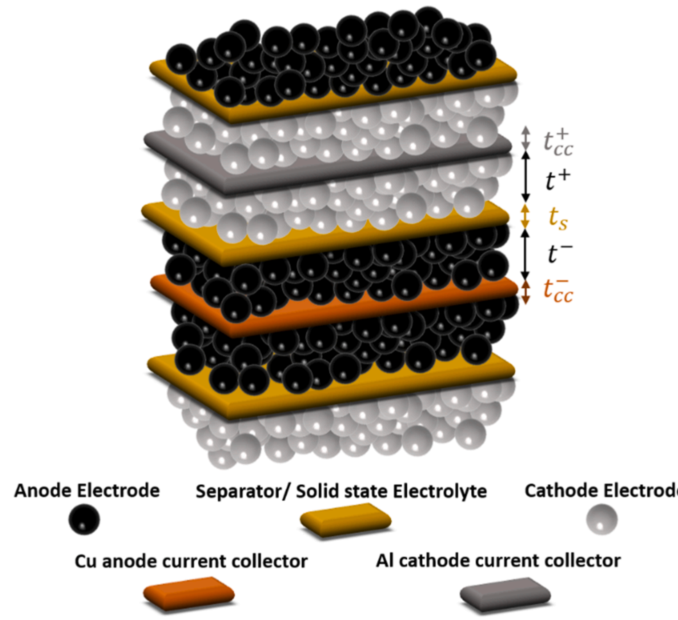

Fig. 1. Schematic of stacked electrodes and separator/solid-state electrolyte to show the thickness used for the equation, t_{cc}^{+} and t_{cc}^{-} are the thickness of cathode and anode current collector, *t+* and *t-* are the thickness of cathode and anode, and ts is thickness of separator.

Table 1
Parameters used for the simulation.

Electrode	NMC with catholyte	Commercial NMC electrodes	Li anode	Graphite
Active Material Density (g/mL)	4.77	4.77	0.53	2.26
$V_{average}$ (V)	3.7	3.7	0	0.125
Specific Gravimetric Capacity (mAh/g)	163	163	3860	350
Percentage of initial irreversible capacity (%)	6.0	6.0	6.0	6.0
Active material volume (%)	60	80	100	60
Thickness of coating (µm)	70	70	18	81
Thickness of current collector(µm)	15	15	15	15
N/P	–	–	1	1.1
Stack Energy Density (Wh/L)	–	–	1326[1]	729[2]

[1] Based on NMC/Li with 20 µm SE.
[2] Based on NMC/Graphite with 20 µm SE.

life and reversibility is assumed to be similar with the commercial battery.

$$\breve{U}_R = \frac{2\tilde{q}_R^+ t^+}{t_{cc}^+ + t_{cc}^- + 2t_s + 2t^+\left[1+\frac{\tilde{q}_R^+\varphi_0^-}{\tilde{q}_R^-\varphi_0^+}\left(\frac{N}{P}\right)\right]}\left(V_{avg}^+ - V_{avg}^-\right) \quad (1)$$

Where:
Constants
t_{cc}^+ *and* t_{cc}^-: Thickness of anode and cathode current collector
Parameters
t^+: Thickness of cathode t_s: Thickness of separator
$\tilde{q}_R^+$ and $\tilde{q}_R^-$: Volumetric reversible capacity of anode and cathode
φ_0^+ *and* φ_0^-: Initial Coulombic efficiency of anode and cathode
N/P: Negative to positive capacity ratio
V_{avg}^+ *and* V_{avg}^-: Average voltage of anode and cathode

$$\tilde{q}_R = \rho_{AM} \times RC \times V_{AM} \quad (2)$$

$\tilde{q}_R$: Volumetric reversible capacity of the anode or cathode
RC: Reversible capacity of the anode or cathode
V_{AM}: Percent volume of active material in the anode or cathode

2. Results and discussion

Fig. 2a shows the percent improvement of the stack energy density as N/P changes with different thicknesses of SE. All performances were compared with the NMC cathode and graphite anode. Three different thicknesses of SE were considered: 20, 50, and 100 µm to study the change in percent improvement compared to an NMC cathode and a graphite anode. Even though ionic conductivity is an important factor in SE performance, it was not considered in the evaluation since the energy density is a function of the materials' capacity and potential. As a result, we have assumed the ionic conductivity of the SE to be similar to LEs. 20 µm is the thickness of the separator in a commercial battery, where the target of the SE should be to match or surpass the performance of the LE batteries. 50 µm is the thickness where a SE can be prepared as a free-standing film using tape casting. It is likely a thinner electrolyte could be produced with process optimization, but 50 µm was selected for comparison to see what improvements we could observe. Finally, 100 µm is compared since the minimum possible thickness of the SE could be prepared by cutting a disc from films/pellets that are currently tested in lab-scale batteries for proof-of-concept. The highest percent improvement was achieved with an N/P ratio of 0 for all three SE thicknesses. A maximum percent improvement of 130% was achieved with a thickness of 20 µm. This improvement is very optimistic and also not realistic for three reasons. The commercial battery has an N/P ratio of 1.1 because of the initial irreversible capacity of the graphite anode. [45, 46] As discussed, when lithium metal is used, the lithium metal acts as a reservoir of lithium ions in the cell. [47] Theoretically, it is possible to omit lithium completely. However, when the Coulombic efficiency of lithium metal is considered the cell would need the excess lithium but not as much as N/P to 1.0. [32] Fig. 2b shows the thickness of the lithium as a function of the N/P ratio when 70 µm and 60% cathode active material thickness and volume are used. As shown, due to the high energy density of the lithium, 3.8Ah/g, the thickness of the anode is thin. When N/P is 1

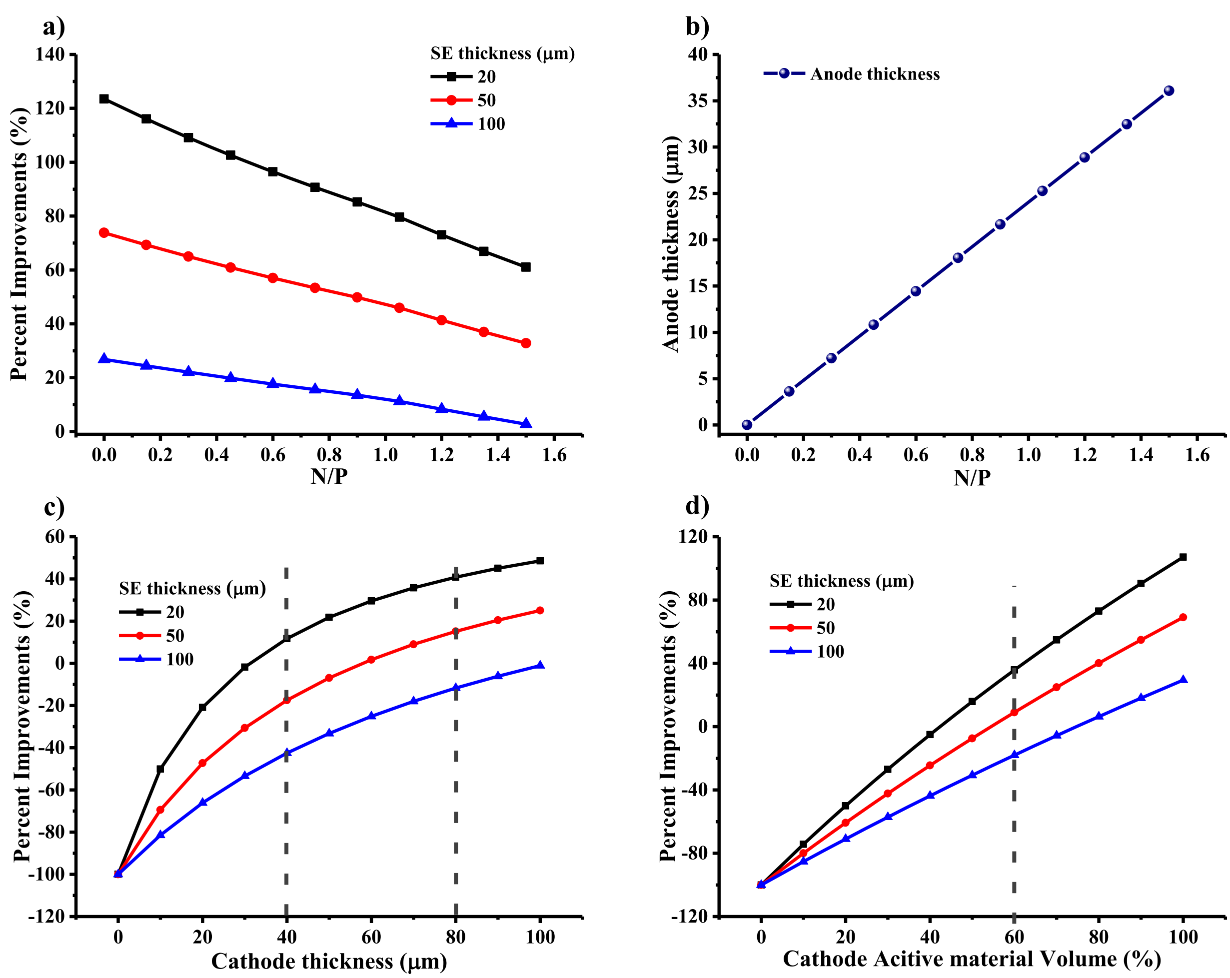

Fig. 2. a) Percent improvement of the stack energy density as N/P changes, b) thickness of anode with N/P c) percent improvement of stack energy density as cathode thickness changes, d) percent improvement of stack energy density as cathode active material volume changes.

the thickness of the lithium becomes 20 μm. This suggests the need for an ultrathin lithium anode, probably less than 50 μm to limit excess lithium to below 190%. [32] The result also emphasizes the need for an anode-free battery to improve energy density. Nevertheless, the anode-free battery also has a lot of challenges ahead. The stability of SEI formation for long cycle life is necessary, which mostly forms during the first cycle. The additive materials to form SEI need to be carefully chosen for ASSBs. Many research was performed on the LE batteries for lithium anode, [47–50] however, most of the salt and solvents will not be required for ASSB. As a result, an additive for in-situ solid-electrolyte interphase formation could be considered to withhold the full cycling life of the battery as in LE, which can also improve the Coulombic efficiency of the lithium metal anode [51]. Optimization of the stack pressure applied to the cell during lithium plating and stripping for high CE is another factor since maintaining high pressure will require additional structural support at the pack level. Furthermore, the anode-free battery will experience close to 20 μmof added lithium plating which is close to a 20% expansion of the total thickness during charging to $2mAh/cm^2$, which is another concern for EV manufacturers. As a result, dense and porous bi or tri-layer solid electrolytes are studied. [52, 53]

Silicon anodes are also considered for next-generation anodes for Li-ion batteries. [54] It has 3.5 Ah/g of practical capacity and there are already some commercial batteries with small amounts of silicon. The silicon anode for ASSBs has several benefits besides the high energy density. However, it still has well-known challenges such as a high volume expansion when lithiated, which results in pulverization with repeated charging and discharging. The repeated volume expansion and contraction also exposes a new surface to the silicon particle that creates solid electrolyte interfaces and result in irreversible capacity when the LE is used. Using solid electrolytes, the SEI formation on the silicon can be minimized due to the solid-solid interaction which can also result in better durability for the silicon anode. [54] Two possible implementations of the silicon can be considered. Silicon as an anode that can result in a 25 μm thick anode or interface materials for the anode-free ASSB. The high specific capacity of the silicon is preferred for SSB compared to graphite anode, but not to the lithium anode since the lithium can be used with a lower N/P ratio. The silicon can act as an interfacial layer between the solid electrolyte and the current collector to protect the solid electrolyte and also improve interface resistance. The application can also lower the N/P ratio, increase overall ASSB energy density and compete with the ultra-thin lithium anode. Furthermore, silicon is abundant and less sensitive to air and moisture which is much easier to process, resulting in lower manufacturing costs.

Fig. 2c shows the change of percent improvement as cathode thickness changes at different SE thicknesses. The results assume the cathode electrodes include SE resulting in 60% active material volume in CAM with an N/P ratio equal to 1. As shown when 100 μm SE is used no improvements can be achieved. It is also important to note, that commercial cathode thickness range from 40 to 80 μm, depending on the high-energy or high-power application purpose. As mentioned before thick cathodes hinder the power density in the LE [42] and SE will have a more profound effect due to the lower ionic conductivity. This suggests that the thinner the SE the higher the energy density. However, due to the challenge of scaling up the process to produce 20 μm SE, it becomes important to improve active material volume in the cathode and optimize N/P by reducing the amount of lithium used as an anode. It should also be pointed out that the SE also requires improvement of the interphases with the cathode and anode, which can also increase the thickness of the SE layers.

Fig. 2d shows improvement in stack energy density as the cathode active material volume changes while the thickness of the cathode is fixed at 70 μm. As shown the improvements are highest when the thickness of the electrolyte is 20 μm. The commercial battery has 95 to 98% of active material in the cathode which represents 80 to 95% active material volume (AV). This represents a 90% improvement with 95% AV and 20 μm SE thickness. However, most of the ASSB battery adds 20wt% SSE to the cathode electrode to provide ionic conductivity that results in 60% AV. With 60% AV, the thickness of the SE needs to be lower than 50 μm to obtain improvement in the stack energy density. The result also shows improving the AV for the cathode provides better performance improvement compared to the thickness of the cathode electrodes.

Fig. 3 shows the percent improvement of the stack energy density when the cathode thickness and active material volume change at three SE thicknesses, 20, 50 and 100 μm. At 100 μm SE thickness the improvements can be 50% when the cathode thickness is 100 μm, but the study from Du et al. [42]. suggests that going over 60 μm will lower the power density due to the diffusion limitation. Also, the active material volume cannot be 100% on the ASSB due to the SE, carbon additives, and binders on the cathode. Devaux et al. [55]. studied a 54 μm thick SE and the maximum cathode thickness without impairing the battery power performance is 48 μm. The needs for the interphase layer on the SE are another important factor. The interfacial layer on the SE lowers interphase resistance and improves the contact between the anode and cathode. Also depending on the SE material, the interfacial layer can protect the SE from lithium metal. The thickness of the layer has not been studied, but based on our studies, the thickness should be part of the SE, which can reduce the actual SE layer to thinner than 20 or 50 μm. This imposes a very difficult challenge to the production of SE. In Fig. 3b, where SE thickness is 50 μm, the energy density starts improving when cathode thickness and CAM volumes are 40 μm and 60% respectively. The limitation of cathode thickness can only be overcome by a decrease in the SE thickness and/or an increase in CAM volume for significant improvement in the energy density. The result implies the importance of catholyte development. Many SE battery includes 10 to 40 wt% of SE in the CAM which corresponds to less than 50% CAM volume. The catholyte in the CAM has many challenges. The amount of catholyte will impact the thickness of the cathode to optimize the energy and power density. The catholyte also needs to have good ionic conductivity to deliver lithium ions to and from the SE. It also needs to have a good interface coating to minimize the interface resistance to lower the overall impedance. Another possible solution to improve the overall energy density can be using the high voltage (5 V) spinel cathode, $LiMn_{1.5}Ni_{0.5}O_4$, LMNO, instead of the conventional $LiNi_{0.33}Mn_{0.33}Co_{0.33}O_2$, NMC 111, and its variants. Based on the calculation when all parameters are the same, due to the higher working potential, 4.7 V, the stack energy density can be improved by up to 82%, which is 20% higher than NMC which is used to evaluate the energy density in this work. However, due to the instability of most SE at high potential, it is difficult to find compatible materials that can last and perform in the battery. Currently, NMC is still challenging due to the instability of the SE over 3.7 V, and many studies are performed using $LiFePO_4$ which has a much lower average voltage of 3.4 V.

Fig. 4 shows the performance improvement as a function of N/P and CAM volume at different SE thicknesses of 20, 50, and 100 μm. Lowest N/P, high CAM volume, and thin SE will provide the biggest improvement as shown in Fig. 4a. However, CAM volume cannot be higher than 95%, due to the carbon additives and polymer binders, especially when the SE is added to the cathode. Much research use 50 to 85 wt% CAM which corresponds to 40 - 75% CAM by volume. This implies that with 100 μm SE thickness, the ASSB will not achieve any improvement in energy density when a 70 μm thick cathode is used. The SE should be at least 50 μm to see the improvement in the energy density. The N/P ratio has a minor effect compared to CAM volume. N/P should be less than 1 to benefit from the high energy density of ASSB and it is only possible when lithium metal is used. To get lower than 1 the manufacturing process needs to be improved since the thickness of the lithium anode becomes less than 25 μm.

Table 2 shows the possible generation of ASSB. Generation 1, GEN 1, can be the current state of the ASSB where the active material in volume, N/P ratio and thickness of SE are set to 60%, 1, and 100 μm, respectively. This results in no improvements, but poor performance. This generation would be better described as a proof of concept only.

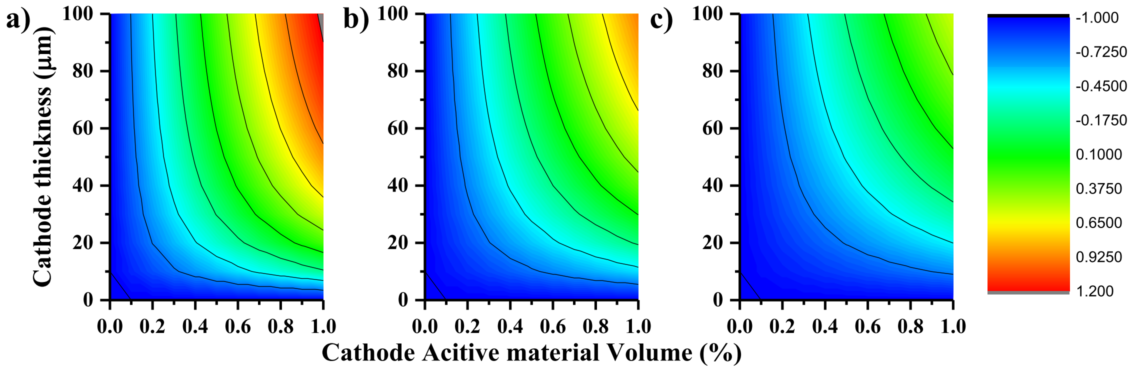

Fig. 3. Performance improvement on cathode thickness and active material volume on three SE thicknesses a) 20 µm, b) 50 µm, and c) 100 µm, N/P ratio = 1.

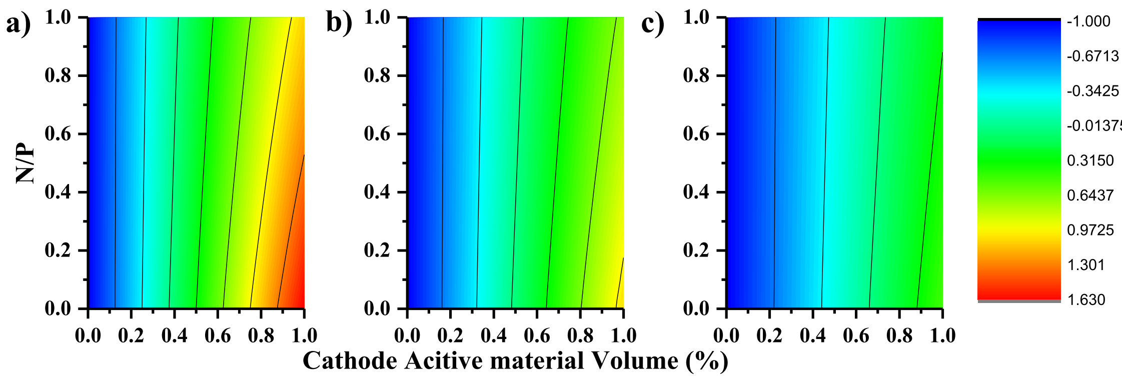

Fig. 4. Performance improvement on cathode thickness and N/P ratio on three SE thicknesses a) 20 µm, b) 50 µm, and c) 100 µm, cathode thickness = 70 µm.

Table 2
Possible strategic target for SSB energy density.

	GEN 1	GEN 2	GEN 3
ACTIVE MATERIAL VOLUME IN CATHODE	60%	70%	80%
N/P RATIO	1	0.5	0
THICKNESS OF SE	100 µm	50 µm	20 µm
PERCENT IMPROVEMENTS IN STACK ENERGY DENSITY	−18%	33%	110%
PERCENT IMPROVEMENT TO THE SYSTEM	N/A	23%	77%

Generation 2, GEN 2, can be the next ASSB where the active material in volume, N/P ratio and thickness of SE are set to 70%, 0.5, and 50 µm, respectively. These factors were determined by considering improvement on the cathode formulation to increase the active material in the cathode, minimizing the amount of lithium in the anode, and thinner fabrication of SE. GEN 2 could be the next commercial ASSB that can be introduced in the near future. This would be the best target with the most recent technological development to achieve 30% higher energy density compared to the current commercial Li-ion battery. With these improvements, it is possible to obtain a 33% increase in the stack energy density. Improving stack energy density does not have equal improvement to the energy storage system as it was shown by Lobberding et al. [56]. that the energy density of the whole system is 60% of that of the cell. When the estimation is considered the energy density improvement for the whole system can be 23%. The final concept generation 3, GEN 3, would be the maximum active material volume in the cathode, anode-free battery, and 20 µm SE same thickness as the commercial separator. This improvement results in 110% and 77% improvement in the stacking and the system energies, respectively. GEN 3 would be the holy grail for the ASSB that can achieve close to a 100% energy density increase. To achieve the GEN 3 battery following parameters should be met and also the challenges would need to be solved.

3. Conclusion

In this study, we have calculated the energy densities of ASSBs using a different set of parameters and compared energy improvements to a baseline of current lithium-ion batteries under different scenarios. By assuming the ionic conductivity of the SE to be the same as the LE, the influence of certain limiting factors (SE thickness, cathode thickness, cathode active material volume, N/P ratio and lithium metal thickness) on the energy density was evaluated. From this study, we found that the SE thickness must be 20 um or less to achieve the highest possible energy improvements. Also, we found that thicker cathodes can provide higher energy density reaching 50% when the cathode thickness is 100 um, but this will have a negative impact on power density. We found that the active material volume in the cathode must reach 80 % which corresponds to the maximum 95% active material weight at the optimized SE and cathode thicknesses, 20 um and 100 um, respectively. However, this target is hard to achieve because of the need for a critical volume of catholyte that is currently way higher than 20% of the cathode formulations. As for the N/P ratio we found that it must be close to 0 that can only be achieved by the use of anode-free or ultrathin lithium anodes. This study demonstrates that are still ongoing challenges that are yet to be overcome before the successful commercialization of All-Solid State Batteries.

Funding information

The authors thank the Office of Energy Research and Development at Natural Resources Canada for financial support.

Declaration of Competing Interest

The authors declare that they have no known competing financial interests or personal relationships that could have appeared to influence the work reported in this paper.

Data availability

No data was used for the research described in the article.

References

[1] S. Randau, D.A. Weber, O. Kötz, R. Koerver, P. Braun, A. Weber, E. Ivers-Tiffée, T. Adermann, J. Kulisch, W.G. Zeier, F.H. Richter, J. Janek, Benchmarking the performance of all-solid-state lithium batteries, Nat. Energy 5 (3) (2020) 259–270, https://doi.org/10.1038/s41560-020-0565-1.

[2] H. Al-Salih, A. Huang, C.-.H. Yim, A.I. Freytag, G.R. Goward, E. Baranova, Y. Abu-Lebdeh, A polymer-rich quaternary composite solid electrolyte for lithium batteries, J. Electrochem. Soc. 167 (7) (2020), 070557, https://doi.org/10.1149/1945-7111/ab7fb8.

[3] S. Abouali, C.-.H. Yim, A. Merati, Y. Abu-Lebdeh, V. Thangadurai, Garnet-based solid-state Li batteries: from materials design to battery architecture, ACS Energy Lett. 6 (5) (2021) 1920–1941.

[4] C. Wang, K. Fu, S.P. Kammampata, D.W. McOwen, A.J. Samson, L. Zhang, G. T. Hitz, A.M. Nolan, E.D. Wachsman, Y. Mo, V. Thangadurai, L. Hu, Garnet-type solid-state electrolytes: materials, interfaces, and batteries, Chem. Rev. 120 (10) (2020) 4257–4300, https://doi.org/10.1021/acs.chemrev.9b00427.

[5] L. Chen, Y. Li, S.-.P. Li, L.-.Z. Fan, C.-.W. Nan, J.B. Goodenough, PEO/garnet composite electrolytes for solid-state lithium batteries: from “ceramic-in-polymer” to “polymer-in-ceramic, Nano Energy 46 (2018) 176–184, https://doi.org/10.1016/j.nanoen.2017.12.037.

[6] J.C. Bachman, S. Muy, A. Grimaud, H.H. Chang, N. Pour, S.F. Lux, O. Paschos, F. Maglia, S. Lupart, P. Lamp, L. Giordano, Y. Shao-Horn, Inorganic solid-state electrolytes for lithium batteries: mechanisms and properties governing ion conduction, Chem. Rev. 116 (1) (2016) 140–162, https://doi.org/10.1021/acs.chemrev.5b00563.

[7] Z. Ma, H.G. Xue, S.P. Guo, Recent achievements on sulfide-type solid electrolytes: crystal structures and electrochemical performance, J. Mater. Sci. 53 (6) (2018) 3927–3938, https://doi.org/10.1007/s10853-017-1827-6.

[8] A. Varzi, R. Raccichini, S. Passerini, B. Scrosati, Challenges and prospects of the role of solid electrolytes in the revitalization of lithium metal batteries, J. Mater. Chem. A 4 (44) (2016) 17251–17259, https://doi.org/10.1039/c6ta07384k.

[9] Y. Zhang, J. Meng, K. Chen, H. Wu, J. Hu, C. Li, Garnet-based solid-state lithium fluoride conversion batteries benefiting from eutectic interlayer of superior wettability, ACS Energy Lett. 5 (4) (2020) 1167–1176, https://doi.org/10.1021/acsenergylett.0c00383.

[10] L. Yang, Q. Dai, L. Liu, D. Shao, K. Luo, S. Jamil, H. Liu, Z. Luo, B. Chang, X. Wang, Rapid sintering method for highly conductive Li7La3Zr2O12 ceramic electrolyte, Ceram. Int. 46 (8) (2020) 10917–10924, https://doi.org/10.1016/j.ceramint.2020.01.106. Part A.

[11] Y. Pang, J. Pan, J. Yang, S. Zheng, C. Wang, Electrolyte/electrode interfaces in all-solid-state lithium batteries: a review, Electrochem. Energy Rev. 4 (2) (2021) 169–193, https://doi.org/10.1007/s41918-020-00092-1.

[12] C.H. Chen, K. Amine, Ionic conductivity, lithium insertion and extraction of lanthanum lithium titanate, Solid State Ionics 144 (1–2) (2001) 51–57, https://doi.org/10.1016/S0167-2738(01)00884-0.

[13] Y.H. Cho, J. Wolfenstine, E. Rangasamy, H. Kim, H. Choe, J. Sakamoto, Mechanical properties of the solid Li-ion conducting electrolyte: li 0.33 La 0.57 TiO 3, J. Mater. Sci. 47 (16) (2012) 5970–5977, https://doi.org/10.1007/s10853-012-6500-5.

[14] M. Wang, J. Sakamoto, Correlating the interface resistance and surface adhesion of the Li metal-solid electrolyte interface, J. Power Sources 377 (2018) 7–11, https://doi.org/10.1016/j.jpowsour.2017.11.078.

[15] P. Hartmann, T. Leichtweiss, M.R. Busche, M. Schneider, M. Reich, J. Sann, P. Adelhelm, J. Janek, Degradation of NASICON-type materials in contact with lithium metal: formation of mixed conducting interphases (MCI) on solid electrolytes, J. Phys. Chem. C 117 (41) (2013) 21064–21074, https://doi.org/10.1021/jp4051275.

[16] M. Keller, A. Varzi, S. Passerini, Hybrid electrolytes for lithium metal batteries, J. Power Sources 392 (2018) 206–225, https://doi.org/10.1016/j.jpowsour.2018.04.099.

[17] Q. Zhang, D. Cao, Y. Ma, A. Natan, P. Aurora, H. Zhu, Sulfide-based solid-state electrolytes: synthesis, stability, and potential for all-solid-state batteries, Adv. Mater. 31 (44) (2019), https://doi.org/10.1002/adma.201901131.

[18] A. Sharafi, E. Kazyak, A.L. Davis, S. Yu, T. Thompson, D.J. Siegel, N.P. Dasgupta, J. Sakamoto, Surface chemistry mechanism of ultra-low interfacial resistance in the solid-state electrolyte Li7La3Zr2O12, Chem. Mater. 29 (18) (2017) 7961–7968, https://doi.org/10.1021/acs.chemmater.7b03002.

[19] M. Echeverri, N. Kim, T. Kyu, Ionic conductivity in relation to ternary phase diagram of poly(ethylene oxide), Succinonitrile, and Lithium Bis(trifluoromethane) sulfonimide blends, Macromolecules 45 (15) (2012) 6068–6077, https://doi.org/10.1021/ma3008509.

[20] M. Armand, M. Duclot, Composition composite de matériau d'électrode et d'un matériau élastomère à conduction ionique et électrode formée à partir de cette composition, French Pat. (1978).

[21] M.B. Armand, J.M. Chabagno, M. Duclot, Second international meeting on solid electrolytes (1978).

[22] M.B. Armand, J.M. Chabagno, M.J. Duclot, Fast ion transport in solids (1979) 131–136.

[23] C. Sun, J. Liu, Y. Gong, D.P. Wilkinson, J. Zhang, Recent advances in all-solid-state rechargeable lithium batteries, Nano Energy 33 (2017) 363–386, https://doi.org/10.1016/j.nanoen.2017.01.028.

[24] S.K. Fullerton-Shirey, J.K. Maranas, Effect of LiClO 4 on the structure and mobility of PEO-based solid polymer electrolytes, Macromolecules 42 (6) (2009) 2142–2156, https://doi.org/10.1021/ma802502u.

[25] J.G. Kim, B. Son, S. Mukherjee, N. Schuppert, A. Bates, O. Kwon, M.J. Choi, H. Y. Chung, S. Park, A review of lithium and non-lithium based solid state batteries, J. Power Sources 282 (2015) 299–322, https://doi.org/10.1016/j.jpowsour.2015.02.054.

[26] S. Bag, C. Zhou, P.J. Kim, V.G. Pol, V. Thangadurai, LiF modified stable flexible PVDF-garnet hybrid electrolyte for high performance all-solid-state Li–S batteries, Energy Storage Mater. 24 (2020) 198–207, https://doi.org/10.1016/j.ensm.2019.08.019.

[27] J. Hu, K. Chen, Z. Yao, C. Li, Unlocking solid-state conversion batteries reinforced by hierarchical microsphere stacked polymer electrolyte, Sci. Bull. 66 (7) (2021) 694–707, https://doi.org/10.1016/j.scib.2020.11.017.

[28] H. An, Q. Liu, J. An, S. Liang, X. Wang, Z. Xu, Y. Tong, H. Huo, N. Sun, Y. Wang, Y. Shi, J. Wang, Coupling two-dimensional fillers with polymer chains in solid polymer electrolyte for room-temperature dendrite-free lithium-metal batteries, Energy Storage Mater. 43 (2021) 358–364, https://doi.org/10.1016/j.ensm.2021.09.019.

[29] J. Wu, L. Yuan, W. Zhang, Z. Li, X. Xie, Y. Huang, Reducing the thickness of solid-state electrolyte membranes for high-energy lithium batteries, Energy Environ. Sci. 14 (1) (2021) 12–36.

[30] W.S. LePage, Y. Chen, E. Kazyak, K.-.H. Chen, A.J. Sanchez, A. Poli, E.M. Arruda, M.D. Thouless, N.P. Dasgupta, Lithium mechanics: roles of strain rate and temperature and implications for lithium metal batteries, J. Electrochem. Soc. 166 (2) (2019) A89–A97, https://doi.org/10.1149/2.0221902jes.

[31] J. Liu, H. Yuan, H. Liu, C.-.Z. Zhao, Y. Lu, X.-.B. Cheng, J.-.Q. Huang, Q. Zhang, Unlocking the failure mechanism of solid state lithium metal batteries, Adv. Energy Mater. 12 (4) (2022), 2100748, https://doi.org/10.1002/aenm.202100748.

[32] S.H. Park, D. Jun, G.H. Lee, S.G. Lee, Y.J. Lee, Toward high-performance anodeless batteries based on controlled lithium metal deposition: a review, J. Mater. Chem. A (2021), https://doi.org/10.1039/D1TA02657G.

[33] T. Li, P. Shi, R. Zhang, H. Liu, X.-.B. Cheng, Q. Zhang, Dendrite-free sandwiched ultrathin lithium metal anode with even lithium plating and stripping behavior, Nano Res. 12 (9) (2019) 2224–2229, https://doi.org/10.1007/s12274-019-2368-x.

[34] B.D. Adams, J. Zheng, X. Ren, W. Xu, J.-.G. Zhang, Accurate determination of coulombic efficiency for lithium metal anodes and lithium metal batteries, Adv. Energy Mater. 8 (7) (2018), 1702097, https://doi.org/10.1002/aenm.201702097.

[35] R. Weber, M. Genovese, A.J. Louli, S. Hames, C. Martin, I.G. Hill, J.R. Dahn, Long cycle life and dendrite-free lithium morphology in anode-free lithium pouch cells enabled by a dual-salt liquid electrolyte, Nat. Energy 4 (8) (2019) 683–689, https://doi.org/10.1038/s41560-019-0428-9.

[36] A.J. Louli, A. Eldesoky, R. Weber, M. Genovese, M. Coon, J. deGooyer, Z. Deng, R. T. White, J. Lee, T. Rodgers, R. Petibon, S. Hy, S.J.H. Cheng, J.R. Dahn, Diagnosing and correcting anode-free cell failure via electrolyte and morphological analysis, Nat. Energy 5 (9) (2020) 693–702, https://doi.org/10.1038/s41560-020-0668-8.

[37] Y.-.G. Lee, S. Fujiki, C. Jung, N. Suzuki, N. Yashiro, R. Omoda, D.-.S. Ko, T. Shiratsuchi, T. Sugimoto, S. Ryu, J.H. Ku, T. Watanabe, Y. Park, Y. Aihara, D. Im, I.T. Han, Publisher correction: high-energy long-cycling all-solid-state lithium metal batteries enabled by silver–carbon composite anodes, Nat. Energy 5 (4) (2020) 348, https://doi.org/10.1038/s41560-020-0604-y. -348.

[38] K. Yan, H.-.W. Lee, T. Gao, G. Zheng, H. Yao, H. Wang, Z. Lu, Y. Zhou, Z. Liang, Z. Liu, S. Chu, Y. Cui, Ultrathin two-dimensional atomic crystals as stable interfacial layer for improvement of lithium metal anode, Nano Lett. 14 (10) (2014) 6016–6022, https://doi.org/10.1021/nl503125u.

[39] B. Zhang, L. Chen, J. Hu, Y. Liu, Y. Liu, Q. Feng, G. Zhu, L.-.Z. Fan, Solid-state lithium metal batteries enabled with high loading composite cathode materials and ceramic-based composite electrolytes, J. Power Sources 442 (2019), 227230, https://doi.org/10.1016/j.jpowsour.2019.227230.

[40] S. Ohta, S. Komagata, J. Seki, T. Saeki, S. Morishita, T. Asaoka, All-solid-state lithium ion battery using garnet-type oxide and Li3BO3 solid electrolytes fabricated by screen-printing, J. Power Sources 238 (2013) 53–56, https://doi.org/10.1016/j.jpowsour.2013.02.073.

[41] H. Al-Salih, M.S.E. Houache, E.A. Baranova, Y. Abu-Lebdeh, Composite cathodes for solid-state lithium batteries: “catholytes” the underrated giants, advanced energy and sustainability research n/a(n/a) 2200032. 10.1002/aesr.202200032.

[42] Z. Du, D.L. Wood, C. Daniel, S. Kalnaus, J. Li, Understanding limiting factors in thick electrode performance as applied to high energy density Li-ion batteries, J. Appl. Electrochem. 47 (3) (2017) 405–415, https://doi.org/10.1007/s10800-017-1047-4.

[43] C.-.H. Yim, S. Niketic, N. Salem, O. Naboka, Y. Abu-Lebdeh, Towards improving the practical energy density of li-ion batteries: optimization and evaluation of silicon:graphite composites in full cells, J. Electrochem. Soc. 164 (1) (2016) A6294–A6302, https://doi.org/10.1149/2.0481701jes.

[44] M.N. Obrovac, V.L. Chevrier, Alloy negative electrodes for li-ion batteries, Chem. Rev. 114 (23) (2014) 11444–11502, https://doi.org/10.1021/cr500207g.

[45] J. Sturman, C.-.H. Yim, E.A. Baranova, Y. Abu-Lebdeh, Communication—design of $LiNi_{0.2}Mn_{0.2}Co_{0.2}Fe_{0.2}Ti_{0.2}O_2$as a high-entropy cathode for lithium-ion batteries guided by machine learning, J. Electrochem. Soc. 168 (5) (2021), 050541, https://doi.org/10.1149/1945-7111/ac00f4.

[46] C.S. Kim, K.M. Jeong, K. Kim, C.W. Yi, Effects of capacity ratios between anode and cathode on electrochemical properties for lithium polymer batteries, Electrochim. Acta 155 (2015) 431–436, https://doi.org/10.1016/j.electacta.2014.12.005.

[47] A.J. Louli, M. Coon, M. Genovese, J. deGooyer, A. Eldesoky, J.R. Dahn, Optimizing cycling conditions for anode-free lithium metal cells, J. Electrochem. Soc. 168 (2) (2021), 020515, https://doi.org/10.1149/1945-7111/abe089.

[48] Z. Xie, Z. Wu, X. An, X. Yue, J. Wang, A. Abudula, G. Guan, Anode-free rechargeable lithium metal batteries: progress and prospects, Energy Storage Mater. 32 (2020) 386–401, https://doi.org/10.1016/j.ensm.2020.07.004.

[49] N.-.W. Li, Y. Shi, Y.-.X. Yin, X.-.X. Zeng, J.-.Y. Li, C.-.J. Li, L.-.J. Wan, R. Wen, Y.-. G. Guo, A flexible solid electrolyte interphase layer for long-life lithium metal anodes, Angewandte Chemie Int. Edition 57 (6) (2018) 1505–1509, https://doi.org/10.1002/anie.201710806.

[50] C. Zou, L. Yang, K. Luo, L. Liu, X. Tao, L. Yi, X. Liu, X. Zhang, X. Wang, Situ formed protective layer: toward a more stable interface between the lithium metal anode and Li6PS5Cl solid electrolyte, ACS Appl. Energy Mater. 5 (7) (2022) 8428–8436, https://doi.org/10.1021/acsaem.2c00971.

[51] J. Liu, R. Xu, C. Yan, H. Yuan, J.-.F. Ding, Y. Xiao, T.-.Q. Yuan, J.-.Q. Huang, In situ regulated solid electrolyte interphase via reactive separators for highly efficient lithium metal batteries, Energy Storage Mater. 30 (2020) 27–33, https://doi.org/10.1016/j.ensm.2020.04.043.

[52] K. Fu, Y. Gong, G.T. Hitz, D.W. McOwen, Y. Li, S. Xu, Y. Wen, L. Zhang, C. Wang, G. Pastel, J. Dai, B. Liu, H. Xie, Y. Yao, E.D. Wachsman, L. Hu, Three-dimensional bilayer garnet solid electrolyte based high energy density lithium metal–sulfur batteries, Energy Environ. Sci. 10 (7) (2017) 1568–1575, https://doi.org/10.1039/C7EE01004D.

[53] M. Lei, S. Fan, Y. Yu, J. Hu, K. Chen, Y. Gu, C. Wu, Y. Zhang, C. Li, NASICON-based solid state Li-Fe-F conversion batteries enabled by multi-interface-compatible sericin protein buffer layer, Energy Storage Mater. 47 (2022) 551–560, https://doi.org/10.1016/j.ensm.2022.02.031.

[54] D.H.S. Tan, Y.-.T. Chen, H. Yang, W. Bao, B. Sreenarayanan, J.-.M. Doux, W. Li, B. Lu, S.-.Y. Ham, B. Sayahpour, J. Scharf, E.A. Wu, G. Deysher, H.E. Han, H.J. Hah, H. Jeong, J.B. Lee, Z. Chen, Y.S. Meng, Carbon-free high-loading silicon anodes enabled by sulfide solid electrolytes, Science 373 (6562) (2021) 1494–1499, https://doi.org/10.1126/science.abg7217.

[55] D. Devaux, H. Leduc, P. Dumaz, M. Lecuyer, M. Deschamps, R. Bouchet, Effect of electrode and electrolyte thicknesses on all-solid-state battery performance analyzed with the sand equation, Front. Energy Res. 7 (2020) 168.

[56] H. Löbberding, S. Wessel, C. Offermanns, M. Kehrer, J. Rother, H. Heimes, A. Kampker, From cell to battery system in bevs: analysis of system packing efficiency and cell types, World Electric Vehicle J. 11 (4) (2020) 77.